Green Chemistry

PAPER

View Article Online
View Journal

Cite this: DOI: 10.1039/c3gc42095g

Heterogeneous ditopic $ZnFe_2O_4$ catalyzed synthesis of 4*H*-pyrans: further conversion to 1,4-DHPs and report of functional group interconversion from amide to ester†

Paramita Das,[a] Arghya Dutta,[b] Asim Bhaumik[b] and Chhanda Mukhopadhyay*[a]

Received 9th October 2013,
Accepted 27th November 2013

DOI: 10.1039/c3gc42095g

www.rsc.org/greenchem

Highly stable, environmentally benign $ZnFe_2O_4$ nanopowder was prepared, characterized and applied in the one-pot, three-component synthesis of 4*H*-pyrans in water. The $ZnFe_2O_4$ catalyst provides both acidic (Fe^{3+}) and basic functionalities (O^{2-}) as the reaction requires. The advantages of this method lie in its simplicity, cost effectiveness, environmental friendliness and easier scaling up for large scale synthesis. Water was exploited both as a reaction medium as well as a medium for synthesis of the catalyst. Moreover, water was the only byproduct. The present report puts forward an application of 4*H*-pyrans for the synthesis of 1,4-DHPs. This is the first attempt towards the synthesis of 4*H*-pyran-3-carboxylate from 4*H*-pyran-3-carboxamide. The corresponding functional group interconversion from amide to ester is rare in organic synthesis.

Introduction

Adaptation of synthetic procedures to the requirements of combinatorial chemistry has always been an essential task to solve.[1] In this context multicomponent reactions (MCRs)[2] provide opportunities to construct the scaffold of natural products and diverse drug-like molecules in a single operation which make the strategy important.[3] As a consequence, MCRs as well as domino or related reactions have gained increased attention.[4] However one aspect of MCRs that has received relatively little attention is their development in aqueous environments.[5] Despite a small number of organic reactions which can be performed in the solid state or solvent-free conditions, these approaches are restricted due to the easy formation of undesired side products and the difficult heat flow control. In this regard, water is nature's reaction medium and constitutes a nonflammable, nonhazardous, nontoxic, uniquely redox-stable, inexpensive solvent.[6] For these reasons, the development of synthetically useful, elegant and convergent MCRs using water as the green reaction medium is of prime interest.

Mixed metal oxide nanoparticles (MMONs) have garnered much attention in recent years and are actively pursued in the development of modern organic synthesis and greener reaction protocols.[7] Catalytic processes based on such mixed metal oxide nanocatalysts are simpler, economically efficient and more environmentally friendly, constituting "green chemistry" that produces only the most desirable products.[8] These MMONs have emerged as sustainable alternatives to conventional materials, as robust, high surface area heterogeneous catalysts, cheap and economical. These nano-sized particles increase the exposed surface area of the active component of the catalyst, thereby enhancing the contact between reactants and the catalyst dramatically and mimicking the homogeneous catalysts. Their insolubility in reaction solvents renders them easily separable from the reaction mixture, which in turn makes the product isolation stage effortless. Notably, the MMONs are better in terms of their catalytic activity than the individual component oxides in various reactions because of their enhanced surface area.[9] Thus, in view of modern catalytic chemistry, MMONs represent one of the most important and widely employed materials in catalysis science.

4*H*-Pyran derivatives represent the key building blocks of many natural products and constitute the core of valuable compounds exhibiting a broad spectrum of biological activities. Certain pyran-based motifs are often found as recurring structures in a variety of natural and biologically relevant products[10] along with photochromic materials.[11] These interesting features have projected the 4*H*-pyran framework as a valuable lead pharmacophore and inspired much effort toward

---

[a] *Department of Chemistry, University of Calcutta, 92 APC Road, Kolkata 700009, India. E-mail: cmukhop@yahoo.co.in; Tel: +91-9433019610*

[b] *Department of Materials Science, Indian Association for the Cultivation of Science, Jadavpur, Kolkata 700 032, India. E-mail: msab@iacs.res.in*

† Electronic supplementary information (ESI) available. CCDC 946297, 946296, 946298 and 946299. For ESI and crystallographic data in CIF or other electronic format see DOI: 10.1039/c3gc42095g

the synthesis of its derivatives.[12] Consequently, the incorporation of the two structural features into interesting motifs, such as pyranocoumarins and 2-amino-4*H*-pyran, may have some significance in the design of new therapeutic agents.[13] Moreover, 4*H*-benzo[*b*]pyrans are also potential calcium channel antagonists, which are structurally similar to biologically active 1,4-dihydropyridines.[14] It is therefore little surprising that an enormous amount of research has been carried out to develop efficient synthetic methods for their assembly.[15]

Thus, based on the above facts and as a part of our research program to develop mild and greener methodologies involving nanoparticle derived catalysts[16] we report herein the application of $ZnFe_2O_4$ nanoparticles for the library synthesis of 4*H*-pyrans.

In light of the numerous applications of 4*H*-pyrans, the present report puts forward an application of nucleophilic vinylic substitution followed by intramolecular cyclization of 4*H*-pyran compounds for the synthesis of 1,4-dihydropyridines that provides easy access to two nitrogen–carbon (N–C) bonds in a single operation.

In this report, an assembly of 88 compounds was synthesized and well characterized by ^{1}H & ^{13}C NMR, 2D NMR, FTIR, elemental analysis and X-ray crystallographic analysis.

Results and discussion

Since we were interested in finding an efficient heterogeneous catalyst for 4*H*-pyran synthesis we therefore, conducted a careful literature survey to fully understand the mechanistic interpretation of 4*H*-pyran formation. We realized that the beforehand reported methodologies overlooked the synergistic effect of the combined use of an acid–base ditopic catalyst since in pyran formation some steps are base catalyzed (Knoevenagel condensation) whereas some others are assisted by an acid (namely the addition, cyclization and dehydration leading to the 4*H*-pyran ring system). Therefore, there is still a need to design a more sustainable protocol to afford functionalized 4*H*-pyran. Again, mixed metal oxides exhibit activity and selectivity superior to those shown by individual oxides. Chemical properties of the active sites can be attuned by mixing an oxide catalyst with another metal oxide, so the interaction between two metal cations is highly critical to catalytic performance. For example, iron oxide possesses a Lewis acidic character[17] whereas zinc oxide enjoys a basic character[18] but mixing iron oxide with zinc oxide to form spinel zinc ferrite ($ZnFe_2O_4$) causes the generation of new active sites having enhanced Lewis acidic as well as basic sites.[17] The Lewis acidic behaviour of $ZnFe_2O_4$ is derived from the strong Lewis acceptor properties of Fe^{3+} of Fe_2O_3. On the other hand the basic character of $ZnFe_2O_4$ is due to the O^{2-} of ZnO. This dual catalytic property of mixed metal oxides makes $ZnFe_2O_4$ nanoparticles very interesting for use as a heterogeneous "*E*" catalyst (Eco-friendly, Efficient and Economic).

For this purpose we have prepared zinc ferrite nanoparticles as described by Sato *et al.*[19] and characterized them by powder X-ray diffraction (XRD), high resolution transmission electron microscopy (HRTEM), EDX with elemental analysis, FTIR, solid state UV spectroscopy, X-ray photoelectron spectroscopy (XPS) and N_2 adsorption analysis. (For the preparation and detailed characterization of the catalyst see ESI†.)

Characterization of the catalyst

XRD analysis. The XRD pattern of the sample obtained by calcining at 800 °C (Fig. S1D, see ESI†) clearly depicts the good-quality polycrystalline nature of the single spinel phase of $ZnFe_2O_4$. The diffraction peaks at 2θ values of 18.0, 30.0, 35.3, 36.9, 42.8, 53.2 and 56.7 assigned to the reflection of the (111), (220), (311), (222), (400), (422) and (511) planes have been indexed to Fd3m cubic spinel structure of $ZnFe_2O_4$. The mean crystallite size (coherent diffraction domain size) was estimated to be 24 nm from the half-maximum full width of the (311) peak by the modified Scherrer formula.

HRTEM and EDX elemental analysis. TEM images of the synthesized $ZnFe_2O_4$ obtained by calcining at 800 °C (Fig. S2, see ESI†) clearly show the uniform formation of $ZnFe_2O_4$ nanoparticles with only one type of particle morphology, indicating the formation of one phase, *i.e.* the spinel structure having dimensions of *ca.* 25–30 nm which is also in accordance with the result calculated using the Scherrer formula. The presence of Zn, Fe and O atoms was observed in the EDX spectrum (Fig. S2d, see ESI†).

FT-IR analysis. The presence of the spinel structure for $ZnFe_2O_4$ was further confirmed by FT-IR spectroscopy (Fig. S3, see ESI†). In the present study, the absorption bands for the synthesized zinc ferrite are in the expected range. No band around 3400 cm^{-1} and 1640 cm^{-1} indicates the absence of any OH vibrations of water molecules resulting from the crystalline spinel phase of $ZnFe_2O_4$. According to Waldron, the high frequency bands around 667 cm^{-1} and 540 cm^{-1} and the low frequency band around 417 cm^{-1} are attributed to that of the tetrahedral and octahedral groups, respectively. Moreover, the low frequency band also appeared in the expected range of 332 cm^{-1}. The peak at 1272 cm^{-1} is due to overtones.

UV spectrum. UV-vis diffuse reflectance spectroscopy of $ZnFe_2O_4$ showed a steep absorption edge (Fig. S4, see ESI†). $ZnFe_2O_4$ is highly photoresponsive in both the UV and visible light ranges (>400 nm) as expected, especially in the wavelength range of 300–500 nm. The dark brown color of $ZnFe_2O_4$ did demonstrate the visible light absorption ability of these materials.

XPS spectrum. From X-ray photoelectron spectroscopy the binding energy of O 1s was found to be 533.8 eV (Fig. S5a, see ESI†). XPS signals at 715.19 and 723.0 eV could be attributed to the Fe $2p_{3/2}$ and Fe $2p_{1/2}$ oxidized states of Fe(III) (Fig. S5b, see ESI†), whereas signals at 1025.56 and 1048.53 eV could be attributed to the Zn $2p_{1/2}$ and Zn $2p_{3/2}$ states of Zn(II) (Fig. S5c, see ESI†). Binding energies of Fe $2p_{3/2}$ and Fe2$p_{1/2}$ states of Fe(III) and Zn $2p_{1/2}$ and Zn $2p_{3/2}$ states of Zn(II) are found to be different from the binding energies of those states in α-Fe_2O_3 and ZnO oxide. These clearly reflect that Zn, Fe and O are not present in the form of individual zinc oxide, ferrous oxide or ferric oxide but as spinel zinc ferrite.

N_2 adsorption analysis. Mixed oxides have greater surface area, smaller particle sizes and higher generation of new catalytic active sites than the corresponding oxide homologues. In the present investigation the surface area of $ZnFe_2O_4$ nanopowder obtained by calcining at 800 °C was 16 m^2 g^{-1} (Fig. S6a, see ESI†). The pore volume and average pore diameter were found to be 0.02 cm^3 g^{-1} and 6.09 nm, respectively (Fig. S6b, see ESI†).

Optimization of the reaction conditions

To optimize the reaction conditions, a series of experiments were conducted with a representative reaction of β-naphthol (**1**) (1 mmol), 4-nitrobenzaldehyde (**2**) (1 mmol) and indane-1,3-dione (**3**) (1 mmol) with the variation of reaction parameters, such as catalyst, reaction temperature, *etc.*, and the results are summarized in Table 1.

It was found that 40 mg of ZnO or MgO NPs as the base catalyst could mainly afford the *ortho*-quinone methides (**5**) (formed by Knoevenagel condensation of β-naphthol with aldehyde) along with a small amount of the target compound (**4h**) (Table 1, entries 1, 2) after 24 h stirring at room temperature. However the starting materials were mostly unaffected by acidic catalysts like Fe_2O_3, TiO_2 and CeO_2 NPs at room temperature (Table 1, entries 4, 5, 6). On the other hand, the use of ZnO in combination with Fe_2O_3 as an acid–base dual catalyst showed a significant improvement in the yield of 4*H*-pyran (**4h**) (73%) at room temperature (Table 1, entry 7). This implies that the initial Knoevenagel condensation is a base catalyzed reaction. Subsequent addition *via* the attack of an active methylene compound (here indane-1,3-dione) on *ortho*-quinone methides (**5**), cyclization and dehydration to afford the desired xanthene are acid catalyzed reactions. Interestingly, carrying out the same experiment with only ZnO NP at 70 °C yielded the desired compound (**4h**) in 80% yield (Table 1, entry 8). This could probably be due to the fact that after Knoevenagel condensation in the presence of ZnO, the addition, cyclization and dehydration steps are assisted at higher temperatures. Therefore, we see that though ZnO/Fe_2O_3 is a good catalyst for carrying out this reaction at room temperature, it leads to a yield that is not as high as that of spinel $ZnFe_2O_4$ NPs (Table 1, entry 9). Albeit other mixed oxide spinel NPs like $ZnTiO_3$ offered quantitative conversion to **4h** (Table 1, entry 14), $ZnFe_2O_4$ was a more attractive alternative since it can be created from cheaper materials available in a common class laboratory. With $ZnFe_2O_4$ as a good catalyst in hand, we next examined whether 40 mg of the catalyst was the optimum quantity for this reaction (Table 1, entry 9).

Table 1 Optimization of reaction conditions for the multicomponent coupling reactions[a]

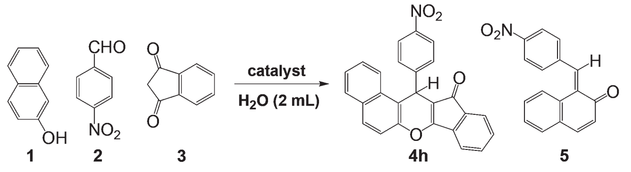

Entry	Catalyst (amount)	Temp.[b] (°C)	Time (h)	Yield[c] (%) 4h	5
1	ZnO NPS (40 mg)	r.t.	24	24	69
2	MgO NPs (40 mg)	r.t.	24	23	68
3	CuO (40 mg)	r.t.	24	—	31
4	Fe_2O_3 (40 mg)	r.t.	24	—	16
5	TiO_2 (40 mg)	r.t.	24	—	18
6	CeO_2 (40 mg)	r.t.	24	—	14
7	ZnO/Fe_2O_3 (40 mg)	r.t.	5	73	14
8	ZnO NPS (40 mg)	70	6	80	12
9	$ZnFe_2O_4$ NPs (40 mg)	r.t.	3	91	—
10	$ZnFe_2O_4$ NPs (20 mg)	r.t.	3	49	—
11	$ZnFe_2O_4$ NPs (10 mg)	r.t.	3	18	—
12	$ZnFe_2O_4$ NPs (5 mg)	r.t.	3	8	—
13	$ZnFe_2O_4$ NPs (50 mg)	r.t.	3	91	—
14	$ZnTiO_3$ NPs (40 mg)	r.t.	3	88	—
15	NaOAc/AcOH (0.2 mmol)	r.t.	8	75	—
16	$NH_4OAc/AcOH$ (0.2 mmol)	r.t.	8	72	—
17	Piperidinium benzoate (0.2 mmol)	r.t.	10	72	—
18	—	r.t.	24	—	—
19[d]	$ZnFe_2O_4$ NPs (3 g)	r.t.	6	82	—

[a] β-Naphthol 1 (1 mmol), 4-nitrobenzaldehyde 2 (1 mmol), indane-1,3-dione 3 (1 mmol), water (2 mL). [b] Here r.t. corresponds to 30 °C. [c] Isolated yields. [d] 150 mmol scale.

Good to excellent conversion was also achieved with different homogeneous catalysts like NaOAc/AcOH, NH_4OAc/AcOH, piperidinium benzoate, *etc.* However, they required repeated work-up, neutralization of acids and bases, and extensive chromatographic purification. Ultimately the isolated yields were not very high (Table 1, entries 15, 16, 17). Therefore, the homogeneous catalysts were replaced with a heterogeneous reusable catalyst. Thus, $ZnFe_2O_4$ was found to be the right choice of catalyst for this particular reaction in generating 4*H*-pyran at room temperature. Importantly, no product was observed without any catalyst (Table 1, entry 18) which further necessitates the use of $ZnFe_2O_4$ in this transformation.

Moreover, this simple procedure allowed easy scale-up of the reaction, and as shown in Table 1, 82% yield was obtained in the 150 mmol scale reaction (Table 1, entry 19), indicating the practicability of our protocol.

Synthetic application of spinel $ZnFe_2O_4$ nanopowder

Synthesis of 2-amino-4*H*-pyrans. With the optimized conditions in hand, to delineate this approach, the scope and generality of this protocol was next examined by employing various aldehydes, carbonyl compounds possessing a reactive α-methylene group and alkylmalonates. An assembly of 44 2-amino-4*H*-pyran compounds was synthesized using this protocol (Scheme 1). Among the aldehydes, aliphatic as well as aromatic aldehydes afforded excellent yields. Aromatic aldehydes with electron-withdrawing as well as electron-donating groups in *o*, *m*, *p* positions of the aromatic ring were converted into desired products in good to excellent yields. It was pleasing to find that acid-sensitive aldehydes (containing heteroatom, methoxy, and hydroxy groups) and highly activated aromatic aldehydes (containing $-NO_2$ groups) also reacted very efficiently with no side reactions. Therefore, the present spinel $ZnFe_2O_4$ nanoparticle catalyzed protocol has general applicability accommodating a variety of substitution patterns. To further expand the scope of the reaction, the use of different alkylmalonates was investigated. To our surprise, all the active methylene compounds (namely malononitrile, ethyl cyanoacetate, methyl cyanoacetate and cyanoacetamide) were easily transformed into the desired products in good to excellent yields. Besides, our methodology has been used successfully with diverse carbonyl compounds possessing a reactive α-methylene group, and corresponding 4*H*-pyrans were obtained in excellent yields without any byproducts. Therefore, this mixed metal oxide catalyst showed an excellent distribution of acid–base sites. The synthetic route is facile, convergent, and allows easy placement of a variety of substituents around the periphery of the heterocyclic ring system. The structures of compounds **7am** and **7ay** were clearly elucidated using X-ray crystallography (Fig. S7 and S8, see ESI†).

Synthesis of the bis-4*H*-pyran system. The rapid generation of molecular complexity in a controlled and predictable manner from simple and readily available starting materials is a contemporary topic in modern organic synthesis. The complexity and brevity mostly rely on the coupling of individual transformations into one synthetic process. In these lines, we speculated that the use of bis-1,4-aldehyde would result in the creation of complex molecules by doubling the efficacy of the above process. The efficiency of this process is further extended to demonstrate the double multicomponent process by utilizing bis-1,3-aldehyde in an analogous manner. The bis-aldehyde was reacted with carbonyl compounds possessing a reactive α-methylene group and alkylmalonates to furnish the respective bis-4*H*-pyran system (Scheme 2). This reaction

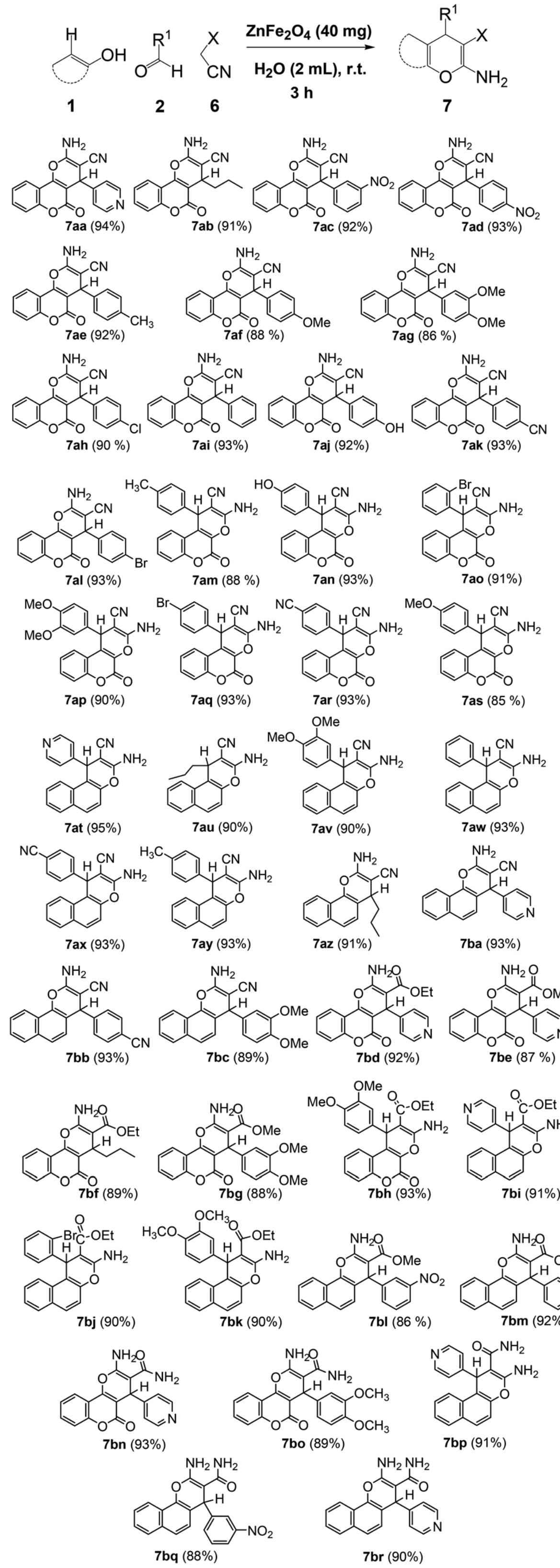

Scheme 1 Library of *4H*-Pyrans synthesized. Reaction conditions: carbonyl compounds possessing a reactive α-methylene group **1** (1 mmol), aldehyde **2** (1 mmol), alkylmalonates **6** (1 mmol), 40 mg of $ZnFe_2O_4$, water (2 mL), 3 h stirring at r.t. (30 °C).

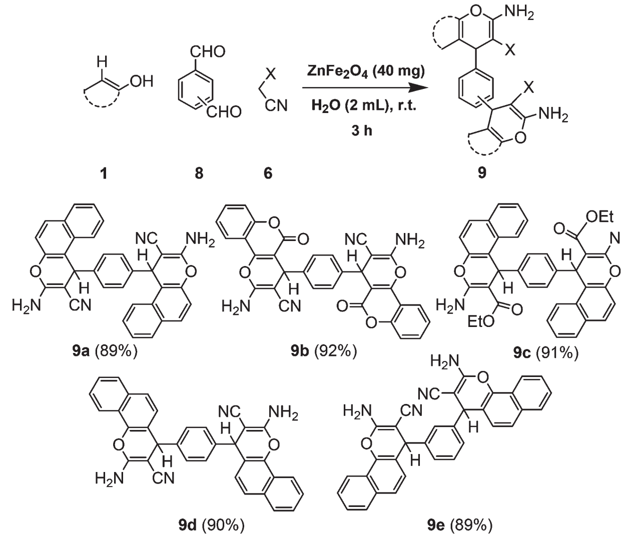

Scheme 2 Scope exploration: generation of bis-*4H*-pyran system. Reaction conditions: carbonyl compounds possessing a reactive α-methylene group **1** (1 mmol), bis-aldehyde **8** (0.5 mmol), alkylmalonates **6** (1 mmol), 40 mg of $ZnFe_2O_4$, water (2 mL), 3 h stirring at r.t. (30 °C).

efficiently resulted in the formation of six chemical bonds, two stereocenters and two 4*H*-pyran units in a single operation. The complex bis-4*H*-pyran systems are skillfully and proficiently synthesized from simple, readily available starting materials.

Synthesis of spiro-4*H*-pyrans. A survey of the literature revealed that albeit the condensation between alkylmalonates, carbonyl compounds possessing reactive α-methylene group and highly reactive ketones (isatin, ninhydrin or acenaphthenequinone) is frequently reported[20] (Scheme 3), to the best of our knowledge to date there has been only one report[21] of spiro-4*H*-pyrans with cyclic aliphatic ketones (cyclopentanone, cyclohexanone, and cycloheptanone) using morpholine as a catalyst with inherent limitations involved in the separation and recycling of the homogeneous catalysts. Therefore, our strategy enabled us to overcome the negative aspects of catalyst leaching in spiro-4*H*-pyrans formation from aliphatic cyclic ketones. To our surprise, despite distinct steric hindrance, ring tension and lower reactivity cyclic ketones reacted smoothly under the present conditions. Both 3- and 4-hydroxycoumarin were totally consumed in this reaction affording moderate to good yield of **13** (Scheme 4). Unlike the reaction with aldehydes, in the reaction with ketones the starting materials were mostly unconsumed with α- and β-naphthol. The low reactivity of ketones in this reaction is also reflected in the reaction temperature since there was only about 15% spiro-4*H*-pyrans formation after stirring the reaction mixture at 30–35 °C for 8 h in water instead of nearly 90% yield at 60–70 °C.

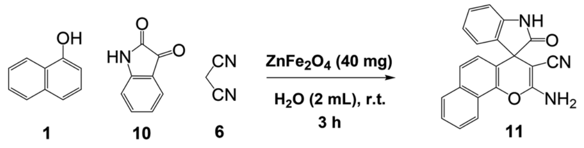

Scheme 3 Synthesis of spirooxindoles **11**. Reaction conditions: carbonyl compounds possessing a reactive α-methylene group **1** (1 mmol), isatin **10** (1 mmol), alkylmalonates **6** (1 mmol), 40 mg of $ZnFe_2O_4$, water (2 mL), 3 h stirring at r.t. (30 °C).

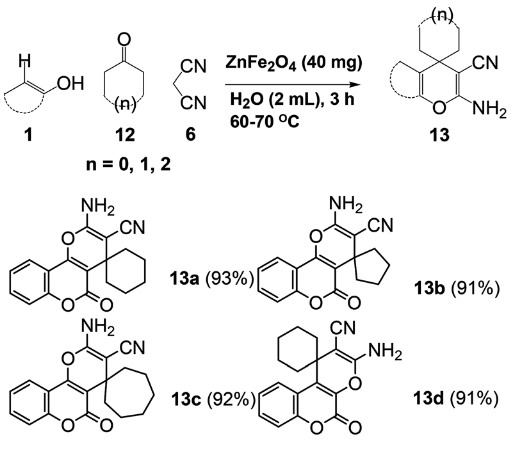

Scheme 4 Formation of spiropyrano[3,2-*c*]chromene using cyclic aliphatic ketones as carbonyl compounds. Reaction conditions: carbonyl compounds possessing a reactive α-methylene group **1** (1 mmol), cyclic aliphatic ketones **12** (1 mmol), alkylmalonates **6** (1 mmol), 40 mg of $ZnFe_2O_4$, water (2 mL), 3 h, 60–70 °C.

Synthesis of benzopyrans. Being inspired by the above results, it was thought worthwhile to replace alkylmalonates with cyclic-1,3-dione in order to show the versatility of this protocol (Scheme 5). For this aim, we have examined the reaction of aldehydes, carbonyl compounds possessing a reactive α-methylene group and dimedone. Notably, a wide range of R^1 groups (aromatic and heteroaromatic) were well tolerated and incorporated. After the successful coupling of carbonyl compounds possessing a reactive α-methylene group **1**, aromatic aldehydes **2** and dimedone, under the same previous reaction conditions, cyclohexane-1,3-dione, 5-phenylcyclohexane-1,3-dione and indane-1,3-dione were also utilized in place of dimedone to show the versatility of this protocol. In this experimentally simple process three new bonds (two C–C and one C–O) and one stereocenter are generated in a single operation with all reactants efficiently utilized.

Synthesis of xanthenes. Xanthenes are biologically important heterocyclic compounds, which possess antiviral anti-inflammatory[22a] and antibacterial activities.[22b] These are being utilized as antagonists for the paralyzing action of zoxazolamine[22c] and in photodynamic therapy.[22d] Furthermore, these compounds can be used as dyes, in laser technologies[22e] and as pH sensitive fluorescent materials for visualization of biomolecules.[22f] As can be seen from Scheme 6, for precursors **2** bearing either electron-donating or electron-withdrawing substituents on the aromatic ring, the reactions all proceeded very smoothly to provide the corresponding xanthene derivatives. The property of substituents on the aromatic ring of the aldehydes did not exert an obvious effect on the reaction yield.

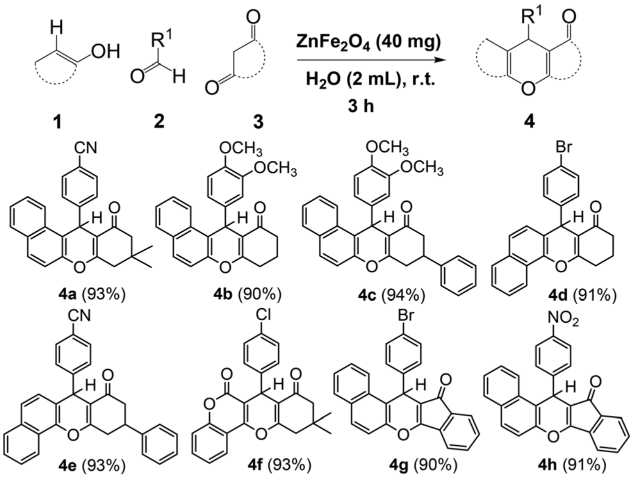

Scheme 5 $ZnFe_2O_4$ nanoparticle catalyzed one-pot synthesis of benzoxanthenes. Reaction conditions: carbonyl compounds possessing a reactive α-methylene group **1** (1 mmol), aldehyde **2** (1 mmol), cyclic-1,3-dione **3** (1 mmol), 40 mg of $ZnFe_2O_4$, water (2 mL), 3 h stirring at r.t. (30 °C).

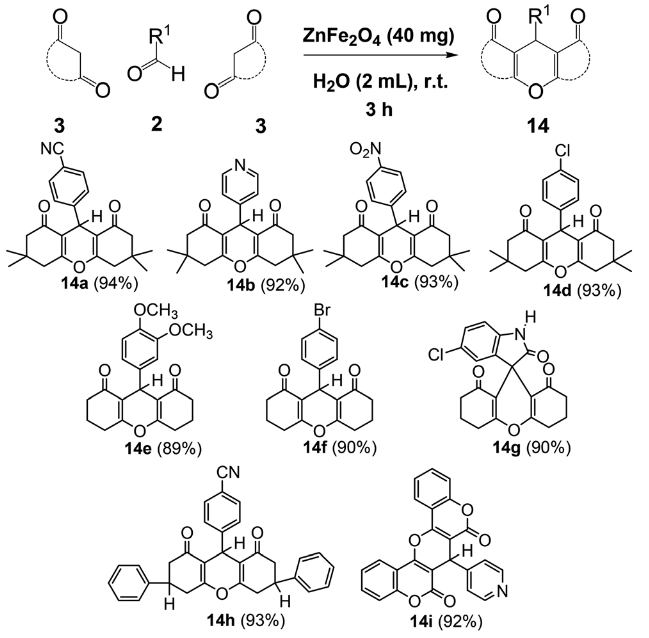

Scheme 6 $ZnFe_2O_4$ nanoparticle catalyzed efficient protocol for xanthene synthesis. Reaction conditions: aldehyde **2** (1 mmol), cyclic-1,3-dione **3** (2 mmol), 40 mg of $ZnFe_2O_4$, water (2 mL), 3 h stirring at r.t. (30 °C).

Our attempt to use isatin as a carbonyl group in this MCR was also successful attesting to the flexibility of the present protocol.

Application of the compounds

One-step synthesis of 1,4-DHPs from xanthenes. 1,4-Dihydropyridines (1,4-DHPs) have potential pharmaceutical activities and could be used as antimalarial, vasodilator, anesthetic, anticovulsant, antiepileptic, and antitumor; and as agrochemical such as fungicide, pesticide, and herbicide.[23] In light of their potential versatility as active determining building blocks of some biologically active natural products, the present report puts forward an application[24] of nucleophilic vinylic substitution (S_NV) followed by intramolecular cyclization of 4*H*-pyran compounds for the one-step synthesis of 1,4-DHPs that provides easy access to two nitrogen–carbon (N–C) bonds in a single operation (Scheme 7). We have confirmed the structure of compound (**16a**) unambiguously by X-ray crystallographic analysis (CCDC 946299) (Fig. S14, see ESI†).

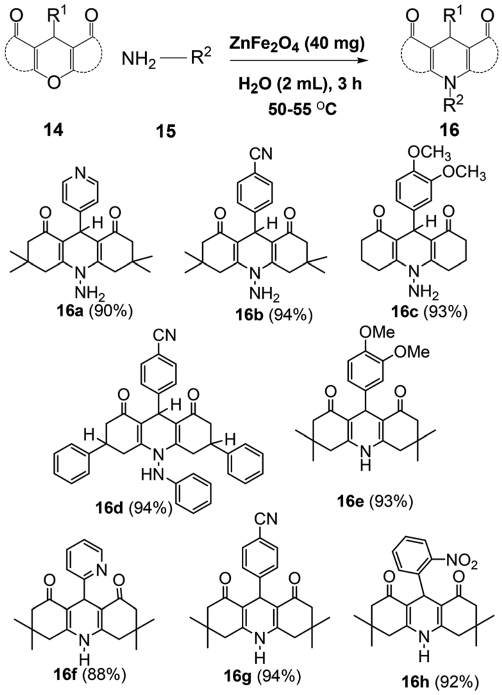

Scheme 7 Synthetic transformation of xanthene to 1,4-DHPs. Reaction conditions: xanthenes **14** (1 mmol), nitrogen-centered nucleophile **15** (1 mmol), 40 mg of $ZnFe_2O_4$, water (2 mL), 3 h, 50–55 °C.

Functional group interconversion from amide to ester. Previous synthetic methodologies for the construction of a 4*H*-pyran scaffold have focused primarily on the combination of carbonyl compounds possessing a reactive α-methylene group, aldehyde and active methylene compounds (namely propanedinitrile, cyanoacetamide and alkyl cyanoacetate). However a synthesis involving alkyl cyanoacetate suffers from limited variety because of the limited availability of the alkyl group of the starting alkyl cyanoacetate (namely methyl and ethyl groups). Although other active methylene groups are commercially available, their use is limited due to their high price. When a precursor that is either commercially not available or less available is used, the E-factor of synthesizing 4*H*-pyran will be increased. In order to circumvent these problems, a general, efficient, and environmentally benign method for synthesizing 4*H*-pyran-3-carboxylate with a wide range of alkyl substituents of the ester group is required. Moreover, the amide substituents in the 3-positions of the pyran ring are quite reactive; this makes these compounds good candidates as precursors for further synthetic transformations to meet the need for various useful purposes. In the presence of a catalytic amount of $ZnFe_2O_4$, a functional group transformation of carboxamides with ester was achieved (Scheme 8). A mechanistic scheme for the conversion of amide to ester is depicted herein for clarity (Scheme 9). Here probably Fe^{3+} remaining in the octahedral holes of $ZnFe_2O_4$ coordinates with the carbonyl carbon of amide increasing its electrophilicity and thereby facilitates the attack of alcohol (R^2OH) on the amide carbonyl carbon. It has been established that structurally $ZnFe_2O_4$ is a normal spinel where it can be written as $(Zn^{2+})(Fe^{3+})_2(O^{2-})_4$. In the $ZnFe_2O_4$ spinel structure Fe^{3+} ions occupy the octahedral holes defined by the O^{2-} ions whereas Zn^{2+} remains in the tetrahedral holes defined by the O^{2-} ions.[25] Thus in $ZnFe_2O_4$ the O^{2-} ions remaining in the lattice site in the $ZnFe_2O_4$ spinel act as a base in the reaction. As shown in Scheme 9, in the third step O^{2-} remaining in the lattice site in $ZnFe_2O_4$ acting as a base abstracts proton from intermediate **20** and produces the target compound **18** after elimination of NH_3. The functional group interconversion from amide to

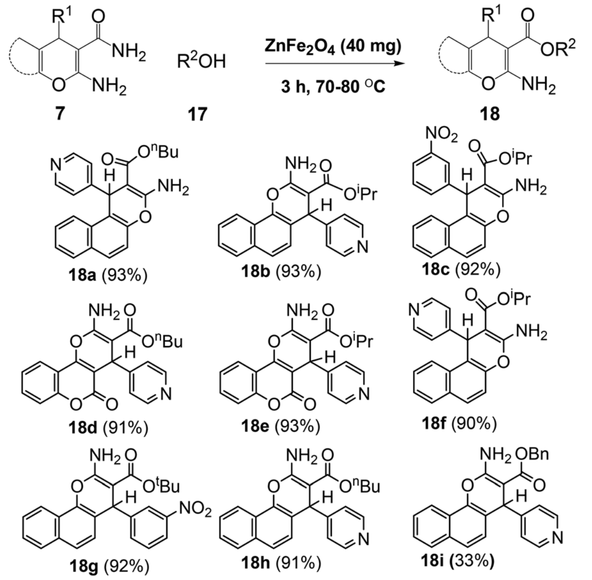

Scheme 8 Synthetic transformation of *4H*-pyran-3-carboxamide to *4H*-pyran-3-carboxylate. Reaction conditions: *4H*-pyran-3-carboxamide **7** (1 mmol), 40 mg of $ZnFe_2O_4$, alcohol **17** (2 mL), 3 h, 70–80 °C.

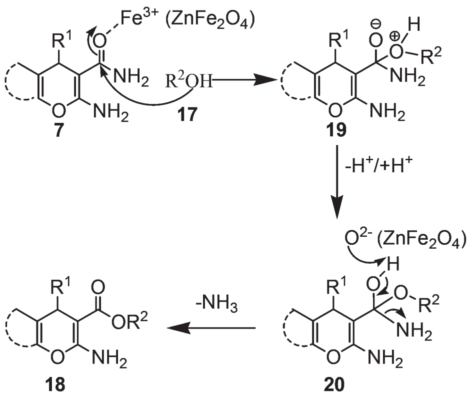

Scheme 9 A plausible reaction scenario to explain the conversion of amide to ester.

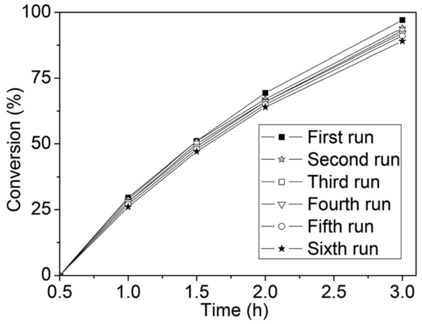

Fig. 1 The reusability of $ZnFe_2O_4$ for the reaction of α-naphthol **1** (1 mmol), pyridine-4-aldehyde **2** (1 mmol), ethyl cyanoacetate **3** (1 mmol) in water (2 mL) at r.t. (30 °C) for 3 h.

ester is compatible with a wide range of alcohols. This observation is rare and very interesting in organic chemistry. In this reaction, the alcohol is not only playing the role of a solvent, but also taking part in the reaction as a reagent. Therefore, we disclose the successful outcome of this endeavor in which a new class of densely substituted 4*H*-pyran-3-carboxylates was prepared in good to excellent yield from 4*H*-pyran-3-carboxamide.

Catalyst stability and recyclability

In order to validate the recyclability of the current $ZnFe_2O_4$ nanopowder catalyst, the re-use investigation was performed in a model reaction of α-naphthol (**1**) (1 mmol), pyridine-4-aldehyde (**2**) (1 mmol) and ethyl cyanoacetate (**3**) (1 mmol) and the $ZnFe_2O_4$ nanopowder catalyst (40 mg) in H_2O (2 mL) for 3 h at r.t. producing **7bm**.

A nearly quantitative catalyst (up to 98%) could be recovered from each run. In a test of six cycles, the catalyst could be reused without significant loss of catalytic activity (Fig. 1). The slight reduction in yield is probably due to the loss of some catalyst at the time of filtration. The recovered catalyst after six runs had no obvious change in structure according to the FT-IR spectrum in comparison with the fresh catalyst (Fig. S11, see ESI†). The XRD observation of the recovered catalyst was also made and there was no obvious change in morphology (Fig. S12, see ESI†). In order to prove that the reaction is heterogeneous, a standard leaching experiment was conducted by means of XPS analysis. β-Naphthol, 4-nitrobenzaldehyde and indane-1,3-dione were allowed to react for 15–20 minutes in the presence of $ZnFe_2O_4$ at room temperature. After this 15–20 minutes period, the reaction mixture was filtered (hot). The filtered reaction mixture was then stirred without a catalyst for the next 12 h; no formation of the corresponding product was observed, indicating that no homogeneous catalyst was involved. XPS analysis of the filtrate (hot) revealed the absence of Fe and Zn species in the filtrate. These results revealed that the metal ions are not leached into the solvent.

Conclusions

In conclusion, $ZnFe_2O_4$ nanopowder performs efficiently as a recyclable ditopic heterogeneous catalytic system for the one-pot construction of the 4*H*-pyran moiety in aqueous media. In the present instance the dual catalytic activity of $ZnFe_2O_4$ was essential for the room temperature synthesis of 4*H*-pyran with a shorter reaction time. Indeed, to the best of our knowledge there are no previous reports on the library synthesis of 4*H*-pyran in the presence of a mixed metal oxide nanocatalyst having both acidic and basic character. The present report puts forward an application of 4*H*-pyran compounds for the synthesis of 1,4-DHPs. In particular an attractive feature of this report is the functional group interconversion from amide of 4*H*-pyran-3-carboxamide to ester leading to 4*H*-pyran-3-carboxylate.

Experimental

General procedure for the synthesis of 7aa–7br

Carbonyl compounds possessing a reactive α-methylene group **1** (1 mmol), aldehyde **2** (1 mmol), alkylmalonates **6** (1 mmol) and 40 mg of $ZnFe_2O_4$ nanopowder catalyst obtained by calcining at 800 °C were added to 2 mL water and the reaction mixture was stirred at r.t. for 3 h. After completion of the reactions (monitored by disappearance of the starting material in thin layer chromatography), ethyl acetate (5 mL) was added to the whole reaction mixture and the solid catalyst was separated from the mixture by filtering through a sinter funnel. The recovered catalyst was washed several times with water and then acetone, dried in a desiccator and stored for another consecutive reaction run. Organic compounds were afforded by evaporation of the solvent in a rotary evaporator and the solid residue was finally recrystallized from ethyl acetate–pet. ether. The products were characterized by standard analytical techniques such as ^{1}H & ^{13}C NMR, 2D NMR, FTIR, elemental analysis, melting point determination, and X-ray crystallographic analysis and all gave satisfactory results.

General synthetic procedure for the preparation of 9a–9e

Carbonyl compounds possessing a reactive α-methylene group **1** (1 mmol), bis-1,4 and bis-1,3-aldehyde **8** (0.5 mmol), alkylmalonates **6** (1 mmol) and 40 mg of the $ZnFe_2O_4$ nanopowder catalyst obtained by calcining at 800 °C were added to 2 mL water and the reaction mixture was stirred at r.t. for 3 h. After completion of the reactions (monitored by disappearance of the starting material in thin layer chromatography), ethyl acetate (5 mL) was added to the whole reaction mixture and the solid catalyst was separated from the mixture by filtering through a sinter funnel. The recovered catalyst was washed several times with water and then acetone, dried in a desiccator and stored for another consecutive reaction run. Organic compounds were afforded by evaporation of the solvent in a rotary evaporator and the solid residue was finally recrystallized from ethyl acetate–pet. ether. The products were characterized by standard analytical techniques such as ^{1}H & ^{13}C NMR, FTIR, elemental analysis, and melting point determination and all gave satisfactory results.

General synthetic procedure for the preparation of 11

Carbonyl compounds possessing a reactive α-methylene group **1** (1 mmol), isatin **10** (1 mmol), alkylmalonates **6** (1 mmol) and 40 mg of $ZnFe_2O_4$ nanopowder catalyst obtained by calcining at 800 °C were added to 2 mL water and the reaction mixture was stirred at r.t. for 3 h. After completion of the reactions (monitored by disappearance of the starting material in thin layer chromatography), ethyl acetate (5 mL) was added to the whole reaction mixture and the solid catalyst was separated from the mixture by filtering through a sinter funnel. The recovered catalyst was washed several times with water and then acetone, dried in a desiccator and stored for another consecutive reaction run. Organic compounds were afforded by evaporation of the solvent in a rotary evaporator and the solid residue was finally recrystallized from ethyl acetate–pet. ether. The products were characterized by standard analytical techniques such as ^{1}H & ^{13}C NMR, FTIR, elemental analysis, and melting point determination and all gave satisfactory results.

General synthetic procedure for the preparation of 13a–13d

Carbonyl compounds possessing a reactive α-methylene group **1** (1 mmol), cyclic aliphatic ketones **12** (1 mmol), alkylmalonates **6** (1 mmol) and 40 mg of the $ZnFe_2O_4$ nanopowder catalyst obtained by calcining at 800 °C in water were heated at 60–70 °C for 3 h. After completion of the reactions (monitored by disappearance of the starting material in thin layer chromatography), ethyl acetate (5 mL) was added to the whole reaction mixture and the solid catalyst was separated from the mixture by filtering through a sinter funnel. The recovered catalyst was washed several times with water and then acetone, dried in a desiccator and stored for another consecutive reaction run. Pure organic compounds were afforded by evaporation of the solvent in a rotary evaporator and the crude product was further purified by silica gel column chromatography using ethyl acetate–petroleum ether as an eluent. The products were characterized by standard analytical techniques such as ^{1}H & ^{13}C NMR, FTIR, elemental analysis, and melting point determination and all gave satisfactory results.

General procedure for the synthesis of 4a–4h

Carbonyl compounds possessing a reactive α-methylene group **1** (1 mmol), aldehyde **2** (1 mmol), cyclic-1,3-dione **3** (1 mmol) and 40 mg of $ZnFe_2O_4$ nanopowder catalyst obtained by calcining at 800 °C were added to 2 mL water and the reaction mixture was stirred at r.t. for 3 h. After completion of the reactions (monitored by disappearance of the starting material in thin layer chromatography), ethyl acetate (5 mL) was added to the whole reaction mixture and the solid catalyst was separated from the mixture by filtering through a sinter funnel. The recovered catalyst was washed several times with water and then acetone, dried in a desiccator and stored for another consecutive reaction run. Organic compounds were afforded by evaporation of the solvent in a rotary evaporator and the solid residue was finally recrystallized from ethyl acetate–pet. ether. The products were characterized by standard analytical techniques such as ^{1}H & ^{13}C NMR, FTIR, elemental analysis, and melting point determination and all gave satisfactory results. Along with the first intermediate (**5**), another intermediate (2nd) was also isolated, both of which were well characterized by standard analytical techniques such as ^{1}H & ^{13}C NMR, FTIR, elemental analysis, melting point determination and X-ray crystallographic analysis (2nd intermediate).

General synthetic procedure for the synthesis of 14a–14i

Aldehyde **2** (1 mmol), cyclic-1,3-dione **3** (2 mmol) and 40 mg of $ZnFe_2O_4$ nanopowder catalyst obtained by calcining at

800 °C were added to 2 mL water and the reaction mixture was stirred at r.t. for 3 h. After completion of the reactions (monitored by disappearance of the starting material in thin layer chromatography), ethyl acetate (5 mL) was added to the whole reaction mixture and the solid catalyst was separated from the mixture by filtering through a sinter funnel. The recovered catalyst was washed several times with water and then acetone, dried in a desiccator and stored for another consecutive reaction run. Organic compounds were afforded by evaporation of the solvent in a rotary evaporator and the solid residue was finally recrystallized from ethyl acetate–pet. ether. The products were characterized by standard analytical techniques such as ^{1}H & ^{13}C NMR, FTIR, elemental analysis, and melting point determination and all gave satisfactory results.

General procedure for the synthesis of 16a–16h

Xanthenes **14** (1 mmol), nitrogen-centered nucleophile **15** (1 mmol), and 40 mg of $ZnFe_2O_4$ nanopowder catalyst obtained by calcining at 800 °C in water were heated at 50–55 °C for 3 h. After completion of the reactions (monitored by disappearance of the starting material in thin layer chromatography), ethyl acetate (5 mL) was added to the whole reaction mixture and the solid catalyst was separated from the mixture by filtering through a sinter funnel. The recovered catalyst was washed several times with water and then acetone, dried in a desiccator and stored for another consecutive reaction run. Organic compounds were afforded by evaporation of the solvent in a rotary evaporator and the solid residue was finally recrystallized from ethyl acetate–pet. ether. The products were characterized by standard analytical techniques such as ^{1}H & ^{13}C NMR, FTIR, elemental analysis, melting point determination, and X-ray crystallographic analysis and all gave satisfactory results.

General procedure for the synthesis of 18a–18i

4*H*-Pyran-3-carboxamide **7** (1 mmol) and 40 mg of $ZnFe_2O_4$ nanopowder catalyst obtained by calcining at 800 °C were heated at 70–80 °C in various alcohols (2 mL) for 3 h. After completion of the reactions (monitored by disappearance of the starting materials in the thin layer chromatography) the solvent was evaporated and the compound was taken in ethyl acetate (5 mL) and filtered through a sinter funnel to separate the catalyst as residue from the product as filtrate. The recovered catalyst was washed several times with water and then acetone, dried in a desiccator and stored for another consecutive reaction run. Organic compounds were afforded by evaporation of the solvent in a rotary evaporator and the solid residue was finally recrystallized from ethyl acetate–pet. ether. The products were characterized by standard analytical techniques such as ^{1}H & ^{13}C NMR, FTIR, elemental analysis, and melting point determination and all gave satisfactory results.

Procedure for the scale-up synthesis of 4h

β-Naphthol **1** (21.62 g, 150 mmol), 4-nitrobenzaldehyde **2** (22.66 g, 150 mmol), indane-1,3-dione **3** (21.92 g, 150 mmol) and 3 g of $ZnFe_2O_4$ nanopowder catalyst were added to 300 mL water and the reaction mixture was stirred by a mechanical stirrer at r.t. for 6 h. After completion of the reactions, ethyl acetate (300 mL) was added to the whole reaction mixture and the solid catalyst was separated from the mixture by filtering through a sinter funnel. Organic compounds were obtained by evaporation of the solvent in a rotary evaporator and the solid residue was finally recrystallized from ethyl acetate–pet. ether to afford 49.86 g (82%) of product.

Acknowledgements

One of the authors (PD) thanks the Council of Scientific and Industrial Research, New Delhi for her fellowship (SRF). We thank the CAS Instrumentation Facility, Department of Chemistry, University of Calcutta for spectral data. We also acknowledge the grant received from the UGC funded Major project, F. no. 37-398/2009 (SR) dated 11-01-2010.

Notes and references

1 *Combinatorial Chemistry: From Theory to Application*, ed. W. Bannwarth and B. Hinzen, Wiley-VCH, Weinheim, Germany, 2006.

2 (*a*) H. Bienayme, C. Hulme, G. Oddon and P. Schmitt, *Chem.–Eur. J.*, 2000, **6**, 3321; (*b*) S. L. Dax, J. J. McNally and M. A. Youngman, *Curr. Med. Chem.*, 1999, **6**, 255; (*c*) L. F. Tietze and A. Modi, *Med. Res. Rev.*, 2000, **20**, 304; (*d*) C. Mukhopadhyay, P. Das and R. J. Butcher, *Org. Lett.*, 2011, **13**, 4664; (*e*) S. Ray, P. Das, A. Bhaumik, A. Dutta and C. Mukhopadhyay, *Appl. Catal. A.*, 2013, **458**, 183; (*f*) C. Mukhopadhyay and S. Ray, *Tetrahedron*, 2011, **67**, 7936; (*g*) C. Mukhopadhyay and S. Ray, *Tetrahedron Lett.*, 2011, **52**, 6431; (*h*) P. Das, S. Ray and C. Mukhopadhyay, *Org. Lett.*, 2013, **15**, 5622.

3 (*a*) B. D. Bala, S. M. Rajesh and S. Perumal, *Green Chem.*, 2012, **14**, 2484; (*b*) M. Li, B. Zhanga and Y. Gu, *Green Chem.*, 2012, **14**, 2421; (*c*) A. Kumar, M. K. Gupta and M. Kumar, *Green Chem.*, 2012, **14**, 290.

4 (*a*) Y. L. Zhu, S. L. Huang and Y. J. Pan, *Eur. J. Org. Chem.*, 2005, 2354; (*b*) V. A. Chebanov, V. E. Saraev, S. M. Desenko, V. N. Chernenko, I. V. Knyazeva, U. Groth, T. N. Glasnov and C. O. Kappe, *J. Org. Chem.*, 2008, **73**, 5110.

5 (*a*) K. Kumaravel and G. Vasuki, *Curr. Org. Chem.*, 2009, **13**, 1820; (*b*) C. J. Pierce and C. H. Larsen, *Green Chem.*, 2012, **14**, 2672; (*c*) J. E. Andreasen, B. Shimpukade and T. Ulven, *Green Chem.*, 2013, **15**, 336; (*d*) M. S. Singh, G. C. Nandi and S. Samai, *Green Chem.*, 2012, **14**, 447.

6 V. K. Ahluwalia and R. S. Varma, *Green Solvents for Organic Synthesis*, Alpha Science International, Abingdon, U.K., 2009.

7 (*a*) C. Mercier and P. Chabardes, *Heterog. Catal. Fine Chem., III, Stud. Surf. Sci. Catal.*, 1993, **78**, 677; (*b*) Y. Izumi, N. Natsume, H. Takamine, I. Tamaoki and K. Urabe, *Bull. Chem. Soc. Jpn.*, 1989, **62**, 2159; (*c*) K. Tanabe and

W. F. Holderich, *Appl. Catal., A*, 1999, **181**, 399; (*d*) B. M. Reddy and A. Khan, *Catal. Rev. Sci. Eng.*, 2005, **47**, 257; (*e*) R. Narayanan, *Green Chem. Lett. Rev.*, 2012, **5**, 707; (*f*) R. B. N. Baig and R. S. Varma, *Green Chem.*, 2013, **15**, 398; (*g*) M. B. Gawande, V. D. B. Bonifácio, R. S. Varma, I. D. Nogueira, N. Bundaleski, C. A. A. Ghumman, O. M. N. D. Teodorod and P. S. Branco, *Green Chem.*, 2013, **15**, 1226.

8 A. Dandia, V. Parewa, A. K. Jain and K. S. Rathore, *Green Chem.*, 2011, **13**, 2135.

9 (*a*) A. V. Biradar, S. B. Umbarkar and M. K. Dongare, *Appl. Catal., A*, 2005, **285**, 190; (*b*) A. P. Amrute, A. Bordoloi, N. Lucas, K. Palraj and S. B. Halligudi, *Catal. Lett.*, 2008, **126**, 286; (*c*) S. J. Singh and R. V. Jayaram, *Tetrahedron Lett.*, 2008, **49**, 4249; (*d*) M. B. Gawande and R. V. Jayaram, *Catal. Commun.*, 2006, **7**, 931; (*e*) E. Rafiee and S. Eavania, *Green Chem.*, 2011, **13**, 2116.

10 (*a*) Y. Tang, J. Oppenheimer, Z. Song, L. You, X. Zhang and R. P. Hsung, *Tetrahedron*, 2006, **62**, 10785; (*b*) T. C. McKee, R. W. Fuller, C. D. Covington, J. H. Cardellina, R. J. Gulakowski, B. L. Krepps, J. B. McMahon and M. R. Boyd, *J. Nat. Prod.*, 1996, **59**, 754; (*c*) T. C. McKee, C. D. Covington, R. W. Fuller, H. R. Bokesch, S. Young, J. H. Cardellina, M. R. Kadushin, D. D. Soejarto, P. F. Stevens, G. M. Cragg and M. R. Boyd, *J. Nat. Prod.*, 1998, **61**, 1252; (*d*) E. J. Jung, B. H. Park and Y. R. Lee, *Green Chem.*, 2010, **12**, 2003.

11 (*a*) S. Kumar, D. Hernandez, B. Hoa, Y. Lee, J. S. Yang and A. McCurdy, *Org. Lett.*, 2008, **10**, 3761; (*b*) M. Rawat, V. Prutyanov and W. D. Wulff, *J. Am. Chem. Soc.*, 2006, **128**, 11044; (*c*) O. A. Fedorova, F. Maure, A. V. Chebunkova, Y. P. Strokach, T. M. Valova, L. G. Kuzmina, J. A. K. Howard, M. Wenzel, K. Gloe, V. Lokshin and A. Samat, *J. Phys. Org. Chem.*, 2007, **20**, 469; (*d*) S. Delbaer, J.-C. Micheau and G. Vermeersch, *J. Org. Chem.*, 2003, **68**, 8968; (*e*) H. R. Safaei, M. Shekouhy, S. Rahmanpur and A. Shirinfeshan, *Green Chem.*, 2012, **14**, 1696.

12 (*a*) T. Sunazuka, M. Handa, K. Nagai, T. Shirahata, Y. Harigaya, K. Otoguro, I. Kuwajima and S. Ohmura, *Org. Lett.*, 2002, **4**, 367; (*b*) R. P. Hsung, K. P. Cole, L. R. Zehnder, J. Wang, L. L. Wei, X. F. Yang and H. A. Coverdale, *Tetrahedron*, 2003, **59**, 311; (*c*) H. Leutbecher, L. A. D. Williams, H. Rosner and U. Beifuss, *Bioorg. Med. Chem. Lett.*, 2007, **17**, 978.

13 X. Xie, C. Peng, G. He, H. J. Leng, B. Wang, W. Huang and B. Han, *Chem. Commun.*, 2012, **48**, 10487.

14 (*a*) M. Suarez, E. Salfran, Y. Verdecia, E. Ochoa, L. Alba, N. Martin, R. Martinez, M. Quinteiro, C. Seoane, H. Novoa, N. Blaton, O. M. Peeters and C. De Ranter, *Tetrahedron*, 2002, **58**, 953; (*b*) H. T. A. Mohsen, J. Conrad and U. Beifuss, *Green Chem.*, 2012, **14**, 1696.

15 (*a*) T. S. Jin, A. Q. Wang, X. Wang, J. S. Zhang and T. S. Li, *Synlett*, 2004, 871; (*b*) D. Q. Shi, S. Zhang, Q. Y. Zhuang, S. J. Tu and H. W. Hu, *Chin. J. Org. Chem.*, 2003, **23**, 877; (*c*) L. M. Wang, J. H. Shao, H. Tian, Y. H. Wang and B. Liu, *J. Fluorine Chem.*, 2006, **127**, 97; (*d*) S. Balalaie, M. Bararjanian, A. M. Amani and B. Movassagh, *Synlett*, 2006, 263.

16 (*a*) M. Shekouhy and A. Hasaninejad, *Ultrason. Sonochem.*, 2012, **19**, 307; (*b*) A. Hasaninejad, A. Zare, M. Shekouhy and N. Golzar, *Org. Prep. Proced. Int.*, 2011, **43**, 131; (*c*) A. Hasaninejad, A. Zare, M. Shekouhy and J. Ameri-Rad, *J. Comb. Chem.*, 2010, **12**, 844.

17 C. T. Wang and R. J. Willey, *J. Catal.*, 2001, **202**, 211.

18 P. Das, R. J. Butcher and C. Mukhopadhyay, *Green Chem.*, 2012, **14**, 1376.

19 T. Sato, K. Haneda, N. Seki and T. Iijima, *Appl. Phys. A: Solid Surf.*, 1990, **50**, 13.

20 (*a*) G. Shanthi, G. Subbulakshmi and P. T. Perumal, *Tetrahedron*, 2007, **63**, 2057; (*b*) S. L. Zhu, S. J. Jia and Y. Zhang, *Tetrahedron*, 2007, **63**, 9365.

21 A. M. Pansuriya, M. M. Savant, C. V. Bhuva, J. Singh and Y. T. Naliapara, *ARKIVOC*, 2009, **xii**, 254.

22 (*a*) T. Hideo and J. Teruomi, (Sankyo Co.), *Jpn. Patent*, 56005480, 1981; (*b*) J. P. Poupelin, G. Saint-Ruf, O. Foussard-Blanpin, G. Narcisse, G. Uchida-Ernouf and R. Lacroix, *Eur. J. Med. Chem.*, 1978, **13**, 67; (*c*) G. Saint-Ruf, A. De and H. T. Hieu, *Bull. Chim. Ther.*, 1972, **7**, 83; (*d*) R. M. Ion, *Prog. Catal.*, 1997, **2**, 55; (*e*) M. Ahmad, T. A. King, D.-K. Ko, B. H. Cha and J. J. Lee, *J. Phys. D: Appl. Phys.*, 2002, **35**, 1473; (*f*) C. G. Knight and T. Stephens, *Biochem. J.*, 1989, **258**, 683; (*g*) Q. Zhang, H. Su, J. Luo and Y. Wei, *Green Chem.*, 2012, **14**, 201.

23 (*a*) R. F. Affeldt, E. V. Benvenutti and D. Russowsky, *New J. Chem.*, 2012, **36**, 1502; (*b*) B. Loev, M. Goodman, K. Snader, R. Tedeschi and E. Macko, *J. Med. Chem.*, 1974, **17**, 956; (*c*) F. Bossert, H. Meyer and E. Wehinger, *Angew. Chem., Int. Ed. Engl.*, 1981, **20**, 762; (*d*) S. Goldmann and J. Stoltefuss, *Angew. Chem., Int. Ed. Engl.*, 1991, **30**, 1559; (*e*) R. H. Fagard, *J. Clin. Basic Cardiol.*, 1999, **2**, 163; (*f*) K. Ohashi and A. Ebihara, *Cardiovasc. Drug Rev.*, 2007, **14**, 1; (*g*) B. J. Epstein, K. Vogel and B. F. Palmer, *Drugs*, 2007, **67**, 1309; (*h*) I. O. Donkor, X. Zhou, J. Schmidt, K. C. Agrawal and V. Kishore, *Bioorg. Med. Chem.*, 1998, **6**, 563; (*i*) S. Ray, M. Brown, A. Bhaumik, A. Dutta and C. Mukhopadhyay, *Green Chem.*, 2013, **15**, 1910.

24 B. Jiang, W. J. Hao, J. P. Zhang, S. J. Tu and F. Shia, *Org. Biomol. Chem.*, 2009, **7**, 1171.

25 (*a*) M. R. Anantharaman, S. Jagatheesan, K. A. Malini, S. Sindhu, A. Narayanasamy, C. N. Chinnasamy, J. P. Jacobs, S. Reijne, K. Seshan, R. H. H. Smits and H. H. Brongersma, *J. Magn. Magn. Mater.*, 1998, **189**, 83; (*b*) M. Thomas and K. C. George, *Indian J. Pure Appl. Phys.*, 2009, **47**, 81; (*c*) I. Mohai, J. Szépvölgyi, I. Bertóti, M. Mohai, J. Gubicza and T. Ungár, *Solid State Ionics*, 2001, **141**, 163.